Int. j. adv. multidisc. res. stud. 2022; 2(6):747-753

Received: 18-10-2022
Accepted: 28-11-2022

International Journal of Advanced Multidisciplinary Research and Studies

ISSN: 2583-049X

Application of high-resolution aerogravity data for lithostratigraphic and depth characterization of the Anambra Basin, Southeastern Nigeria

[1] Eke Peter Ogochuku, [2] Onyeche Ihuoma Nnabugwu, [3] Ombu Righteous
[1] Associate Professor, Ignatius Ajuru University of Education, Port Harcourt, Nigeria
[2] Postgraduate Student, Ignatius Ajuru University of Education, Port Harcourt, Nigeria
[3] Department of Physics, Federal Polytechnic Ekowe, Bayelsa State, Nigeria

Corresponding Author: **Eke Peter Ogochuku**

Abstract
Aerogravity anomalies in the Anambra Basin, Nigeria, were analysed for lithostratigraphic and depth characterization. The Bouguer gravity data were enhanced, gridded, and the regional anomalies isolated from the residual anomaly by a second-order polynomial fit. The residual anomalies were interpreted by contouring, modelling and depth estimation using inverse and forward modelling and standard Euler deconvolution operation of the Oasis Montaj Software. The contour map shows low gravity values of−19.5 mGal to zero for subsurface formations in the western, central and north-eastern parts of the regions indicating formations with low density mass. High density subsurface formations with gravity values up to 24.1 mgals are found in the northern, south-eastern, eastern and north-eastern parts of the region. The subsurface formation hosts syncline and anticline structures with faults. Sedimentary depths range from 342 m to 9260 km. This also reflects the depth to basement in the region. These sedimentation depths imply favourable hydrocarbon sources and habitats as is common in the country.

Keywords: Basement, Anambra Basin, Inverse and Forward Modelling, Bouguer Gravity Anomaly, Euler Depth Estimate

1. Introduction

The gravity method of geophysical prospecting is a technique of measuring variations in the earth's gravitational field either on land, sea, or air (Mariita, 2010; Dobrine, 2010) [14, 9]. Land and sea surveys are limited to measurements along selected profiles on land or sea while airborne covers both. According to Igwe *et al*. (2018) [12] an airborne or aerogravity exploration enables the geophysicist to optimally design the survey to address the study targets without limitation of ground access. Additional advantage is the rapid rate of data acquisition and its use in populated settings. Relatively, it is a cheap, non-invasive and non-destructive remote sensing method for measuring differences in the earth's gravitational field at specific locations.

Gravity is a potential field, which means it acts at a distance. As a result, it is passive because no artificial energy input is required to acquire data. The strength of the gravitational field is directly proportional to the mass and the density of subsurface materials and these values change along a profile (Al-Saadi and Baban, 2014) [4]. The information from underlying rock densities can be used for interpretation of subsurface formations hence the success of this method is dependent on the different bulk densities (mass) of the earth materials, which cause variations in the measured gravitational field. The depth, geometry, and density that caused the gravity field variations can be determined using a variety of analytical processes. The gravity data for most subsurface formation interpretation is the Bouguer gravity anomaly (Petit *et al*., 2002). It is an aggregate of the regional and residual gravity anomalies within a given area. This anomaly is interpreted in a variety of ways that include manually inspecting the grid or profiles for variations in the gravitational field to more complex methods of separation of the gravity anomaly due to an object of interest from other gravity anomalies. Several applications of the method can be found in the works of; Zhang *et al*. (2015) [33]; Alrefaee (2017) [5]; Eke and Nelson (2020, 2021) [11]; Chouhan (2020) [6]; Chouhan *et al*. (2020) [7]; Njeudjang *et al*. (2020) [15] and Wang *et al*. (2021) [32].

One important role of the method is in the recognition of sedimentary basins (Ali *et al*. 2014) [3] and structures in which hydrocarbons are entrapped (Tschirhart *et al*., 2017) [31]. Usually, basements have higher density contrast compared to the sedimentary formations above it where hydrocarbons commonly occur (Selley and Sonnenberg, 2015) [30]. In the sedimentary basins, basement faults are structurally important because they influence and determine the overall basin architecture, oil and gas traps and groundwater flow patterns.

The Anambra Basin is one of the major basins in Nigeria with potentials for hydrocarbons in its sedimentary section (Oha *et al*., 2016; Obasi *et al*., 2017; Okpoli, 2019) [21, 17, 22]. However, despite several studies in the basin, the input from the gravity method is not much in terms of interpretation of regional basement structures, determination of basement depths, sedimentary thickness, and its hydrocarbon potentials (Olagundoye *et al*., 2021) [23]. Additionally, the basin has not been fully exploited, so structural information on the basement and sedimentary thickness are needed to improve the exploration of these resources. To improve on the available subsurface information in this region, airborne gravity data of the region obtained from BGI is analysed quantitatively to obtain information on structural types, basement sedimentary thickness and hydrocarbon potential of the basin.

Anambra basin is located approximately between longitudes 6 º 30' E and 8º 00'E and latitudes 5º 00'N and 8º 00'N (Fig 1). The basin covers an area of more than 30, 000 km^2 and contains more than 2 km of Cretaceous marine, paralic, and deltaic facies sediments in out-cropping sections that extend into adjacent tectonic basins such as the Abakaliki Trough, the Afikpo Syncline, and the Calabar Flank (Babatunde, 2010; Abubakar, 2014). The Basin is situated at the south-western extremity of the Benue Trough. It is bounded to the west by the Precambrian basement complex rocks of western Nigeria, to the east by the Abakaliki Anticlinorium (Obaje, 2009; Onyekuru *et al*, 2010) [16, 26]. The north and south boundaries of the Anambra Basin are defined by the Niger hinge line and the Niger Delta hinge line, respectively (Odunze and Obi, 2013) [20]. Ekine and Onuoha (2008) [10] recognize the northern boundary of the basin to coincide with the limit of exposure of the Maastrichtian sediments and the southern boundary to be at Onitsha, which is the northernmost limit of the Tertiary-Present Niger Delta Basin.

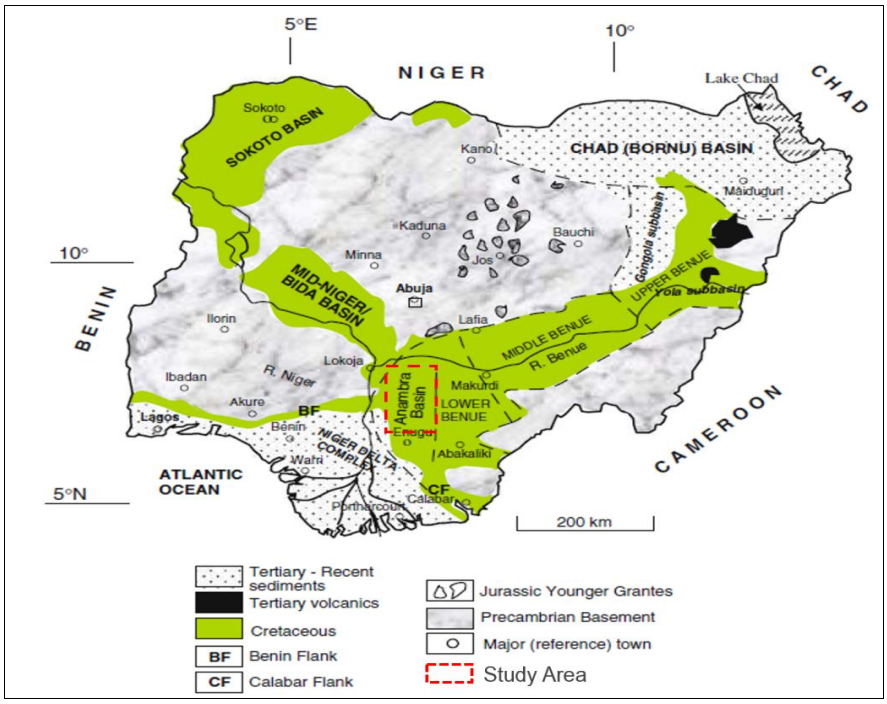

Fig 1: Geological map of Nigeria showing the Anambra Basin which is the study area (Obaje, 2009) [16]

As documented by Obi *et al.* (2001) [18] and Oboh-Ikuenobe *et al.* (2005) [19] sedimentation in the trough was controlled by three major tectonic phases, giving rise to three successive depocenters. The first phase (Albian–Santonian) featured the deposition of the Asu River Group, Eze-Aku and Awgu Formations within the Abakaliki-Benue Trough which was flanked to the east by the Anambra Platform and to the southwest by the Ikpe Platform (Obi *et al*, 2001; Oboh-Ikuenobe *et al*, 2005) [18, 19]. The second phase (Campanian-Eocene) was characterised by compressive movements along the NE-SW axis which resulted in the folding and uplift of the Trough into an anticlinorium. This forced the Anambra Platform to subside and formed the Anambra Basin and the Afikpo Syncline. The deposition of the Nkporo Group, Mamu Formation, Ajali Sandstone, Nsukka Formation, Imo Formation and the Ameki Group then followed. The third sedimentary phase credited for the formation of the petroliferous Niger Delta commenced in the late Eocene as a result of a major earth movement that structurally inverted the Abakaliki region and displaced the Depositional axis further to the Anambra Basin (Obi *et al*, 2001) [18].

The Basin consists of four lithostratigraphic units as reported by Dim *et al*. (2017) [8]. Sedimentation in the began in the Campanian with a short marine transgression depositing the units of the Nkporo Group (Owelli Formation, Nkporo Formation, Enugu Formation), which consists of carbonaceous shales and sandstone members of deltaic origin (Odunze and Obi 2013) [20]. This unit is overlain by the coal-bearing Mamu Formation deposited in the Late Campanian to Early Maastrichtian, at the beginning of a regressive phase. It consists of alternating sandstones, sandy shales and mudstones, with interbedded sub-bituminous coal seams (Akande *et al*., 2007). Overlying the Mamu Formation is the Ajali Formation, which comprises predominantly interbeds of clay laminae and the Nsukka Formation of mid-to-late Maastrichtian age. The Nsukka Formation consists of dark shales and sandstones, with thin coal seams that mark the beginning of the transgression that led into the formation of the Niger Delta Basin in the early

Paleogene (Onuoha and Dim, 2016). The sediment packages were deposited during a regressive cycle (relative sea-level fall) within fluvio-tidal, deltaic, shelfal and marine settings (Dim *et al*. 2017) [8]. Sedimentation thickness of over 9 km has been reported in the region (Olubayo, 2016) [24].

2. Materials and methods

The digitised Bouguer gravity data for this work was obtained from the gravity database of Bureau Gravimetrique International (http://bgi.cnes.fr) covering areas in the Anambra Basin. The zipped data was extracted and enhanced, gridded (Obiora *et al*., 2020) and the regional anomalies separated from the residual anomaly by a second-order polynomial fit before interpretations. Depth estimation was by forward and inverse modelling and Euler depth method using Oasis Montaj Software. To facilitate the application of these Fourier transform (FT)-based techniques and to minimise distortions of the gravity field that is found in the sampling, the gridded data was used to produce maps projected onto Universal Transverse Mercator (UTM). Based on prior knowledge of the depth to basement in the region, a best polynomial fittings based on Mishra (2018) was used to focus on the local and regional anomalies respectively with the regional gravity obtained from the second order polynomial operation,

$$g_R = a_0 + a_1 x + a_2 x^2 + a_3 x^3 .... + a_n x^n \quad (1)$$

The residual anomalies were interpreted by contouring, modelling and Euler deconvolution to estimate the depths to the anomalous bodies from the relation,

$$x\frac{\partial T}{\partial x} + y\frac{\partial T}{\partial y} + z\frac{\partial T}{\partial z} + \eta T = x_0\frac{\partial T}{\partial x} + y_0\frac{\partial T}{\partial y} + z_0\frac{\partial T}{\partial z} + \eta b \quad (2)$$

Where x, y, and z are the coordinates of a measuring point; x_0, y_0 and z_0 are the coordinates of the source location whose total field is detected at x, y, and z; b is a base level; η is structural index (SI) and T is potential field (Adegoke and Layade, 2019; Reid *et al*., 2014) [1, 29]. A contour map interval of 5mGal was constructed and some points selected for inverse and forward modelling.

3. Results and discussions

Fig 2 is the Bouguer base map of the basin with the Bouguer gravity contours and selected portions for modelling. The Bouguer gravity contour depicts the gravity range of -19.9 mGal to 24.1 mGal within the region with arrows indicating the subsurface structural trending in the region.

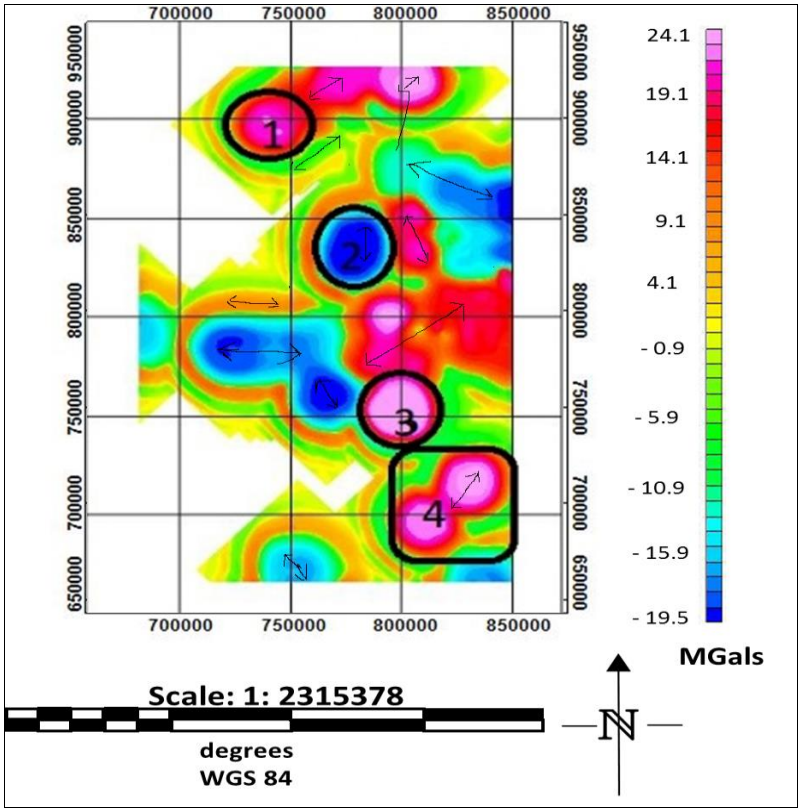

Fig 2: Bouguer gravity grid map showing the locations of four profiles

Fig 3 to 6 are the model results of selected portions 1 to 4 in Fig 3 using sphere and dyke models.

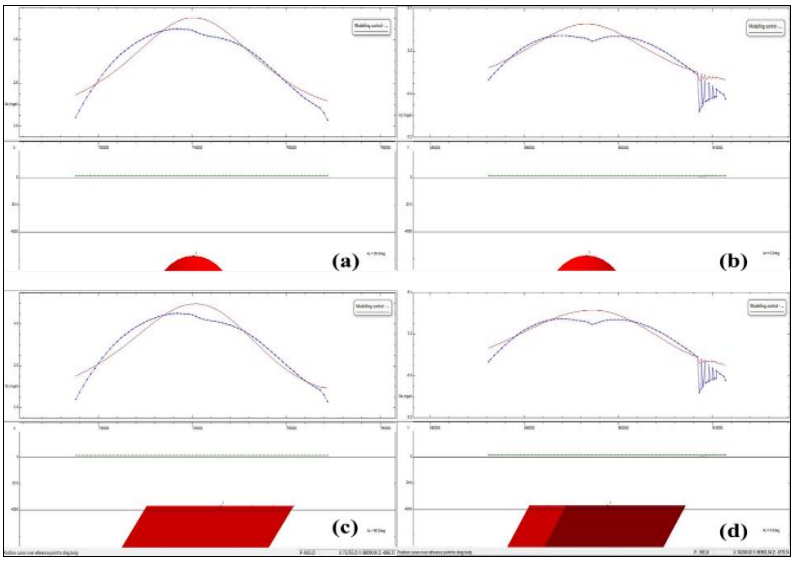

Fig 3: Model result of point 1 (a) Using a sphere model at 90° (b) Using a sphere model at 0° (c) Using a dyke model at 90° (d) using a dyke model at 0°

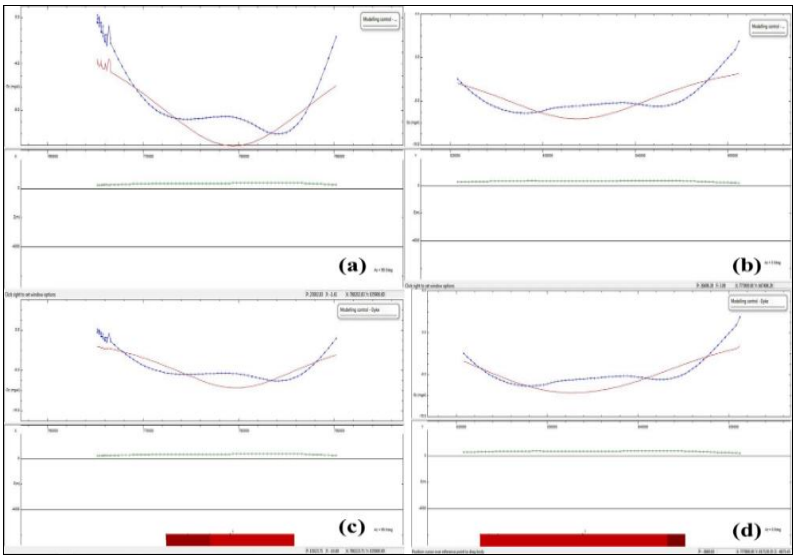

Fig 4: Model result of point 2 (a) Using a sphere model at 90°. (b) Using a sphere model at 0° (c) Using a dyke model at 90° (d) using a dyke model at 0°

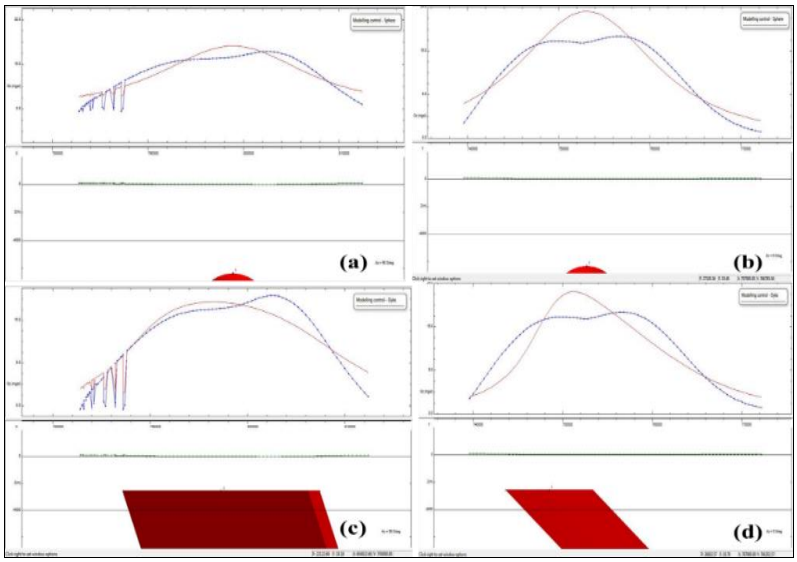

Fig 5: Model result of point 3 (a) Using a sphere model at 90°. (b) Using a sphere model at 0° (c) Using a dyke model at 90° (d) using a dyke model at 0°

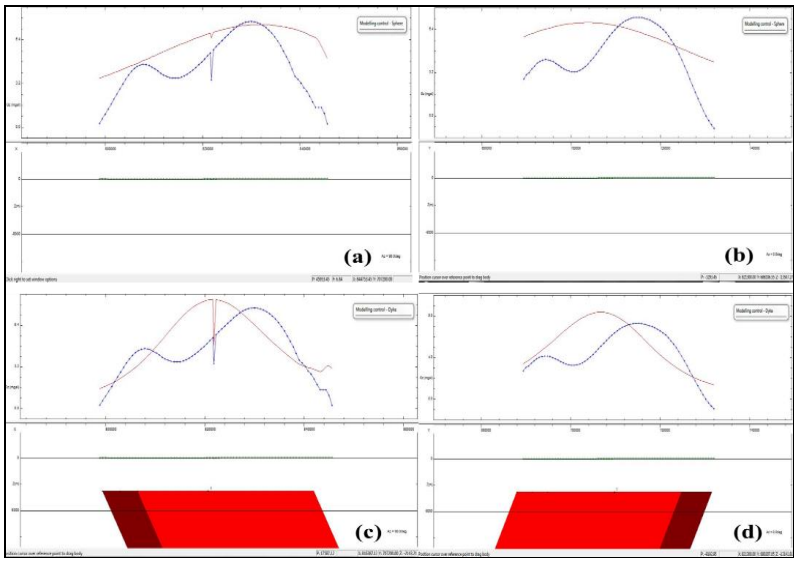

Fig 6: Model result of point 4 (a) Using a sphere model at 90°. (b) Using a sphere model at 0° (c) Using a dyke model at 90° (d) using a dyke model at 0°

Table 1 is a summary of the modelled results for points 1, 2, 3 and 4.

Table 1: Models summary and their respective depths to anomalous bodies

Model	Model Shape	Depth to Anomalous bodies/m	Density contrast of the formations	Root Mean square error	Possible cause of anomaly
1	sphere	5772	0.186	0.552	Anticline \ Faulted Anticline
	dyke	3701	0.083	0.568	
2	sphere	8497	0.487	2.009	Syncline \ Faulted Syncline
	dyke	4978	0.258	1.670	
3	sphere	6358	0.848	2.356	Faulted Anticline
	dyke	2556	0.424	8.546	
4	sphere	2723	0.176	2.595	Faulted Anticline
	dyke	5015	0.073	2.065	

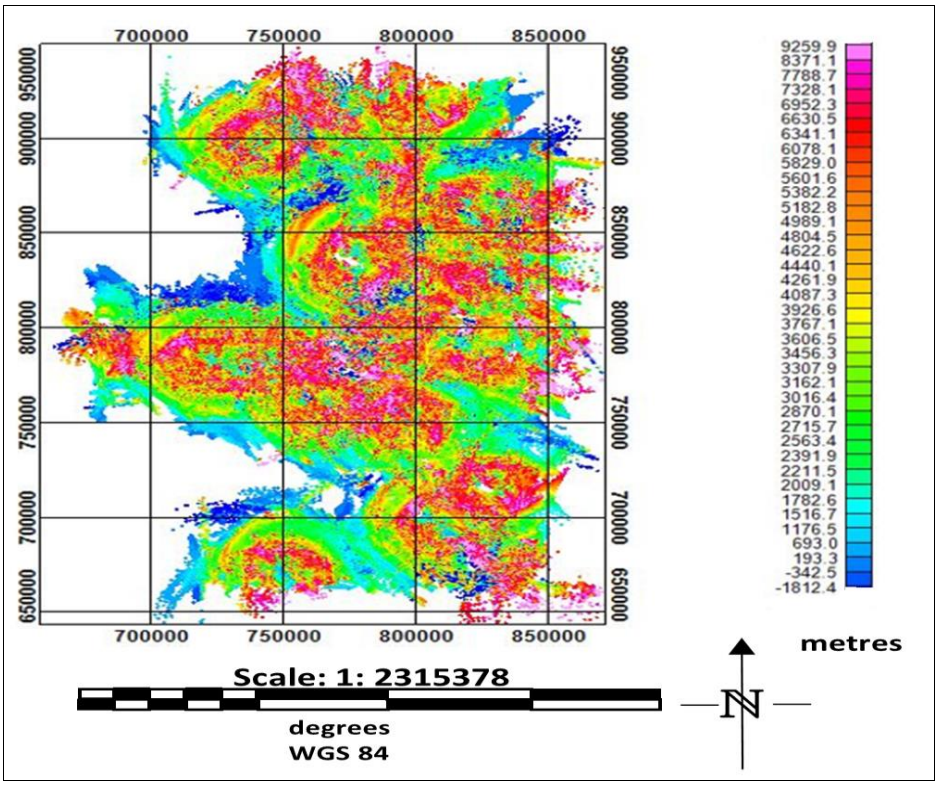

Fig 7: Sediment depth thickness depth range from Euler 3D estimate

The Euler depth estimate from the programme iteration is shown in Fig 7 with sediment thickness range of over 9000 m.

The contour map (Fig 2) shows the subsurface gravity variations and the structural trends in the study area with subsurface structures with low gravity values of between −19.5mGal to zero. These structures can be found in the western, central and north-eastern parts of the regions. These are subsurface formations with low density mass while high density subsurface formations with gravity values up to 24.1 mgals can be found in the northern, south-eastern, eastern and north-eastern parts of the region. The clustering and circular contours are indicative of spherical anomalies attributed to synclines and anticlines bodies (Prieto, 1996) [28], while the long narrow patterns are indicative of dyke related structures modelled in the central, southwestern and northwestern parts of the basin. East-West trending structures can also be found in the western part of the basin, while southwest-northeast trending formations can be found in the southern and northeastern parts of the region.

The model results summarised in Table 1 show anticline and syncline stratigraphic structures with faults. The strike angles suggest strike-slip faults and faulted anticlines which are observed in models 1, 3 and 4, while faulted synclines are observed in model 2. From the results of the modelling, the density contrast (0.073 – 0.848 g/cm3) of the anomalous bodies and sedimentary thickness of 2556 m to 8497 m, the formations are potential hydrocarbon sources and traps. The positive density is an indication that the anomalous body has a higher density than the host rock or surrounding layer while the negative density shows that the anomalous body has a lower density than the surrounding host rock or layer. The positive gravity anomalies are associated with the simple folded symmetrical anticline and normal faulted anticline structures in the region.

The Euler depths estimate (Fig 7) shows that the depth estimates in this region range from 342 m to 9260 m. This is in agreement with the depth ranges from previous works of Adetona and Abu (2013) [2] and Olubayo (2016) [24]. This also implies that the sedimentary depths are favourable for hydrocarbon maturation and generation (Iheanacho, 2010; Olubayo, 2016) [24]. These depths also reflect the depth to the basement in the various parts of the Anambra basin with a maximum depth to basement of 9260 m obtained.

4. Conclusion

This study uses high-resolution aerogravity data to characterise the lithostratigraphy and depth of the Anambra Basin in southeastern Nigeria. The goal of this research was to determine the structural types and sedimentary thickness in the Anambra basin, with implications for hydrocarbon potentials. The findings indicate that low density mass formations are found in the western, central and north-eastern parts of the regions while high density subsurface formations can be found in the northern, south-eastern, eastern and north-eastern parts of the region. Faulted syncline and anticline bodies are found in the southwestern and northwestern parts of the basin with east-west trending structures found in the western part of the basin, while southwest-northeast trending formations can be found in the southern and northeastern parts of the region. The sedimentary thickness and depths to basement range from 342 m to 9260 m in the basin.

5. Acknowledgement

The authors appreciate the International Gravimetric Bureau (Bureau Gravimétrique International (BGI) for gravity data used in this work.

6. Conflict of interest

The authors declare that they have no known conflicting interest.

7. References

1. Adegoke JA, Layade GO. Comparative depth estimation of iron-ore deposit using the Data-Coordinate Interpolation Technique for airborne and ground magnetic survey variation. African Journal of Science, Technology, Innovation and Development (AJSTID). 2019; 11(5):663-669.
2. Adetona AA, Abu M. Estimating the thickness of sedimentation within lower Benue Basin and Anambra Basin, Nigeria, using both spectral determination and source parameter imaging. ISRN Geophysics, 2013, 1-10.
3. Ali MY, Watts AB, Farid A. Gravity anomalies of the United Arab Emirates: Implications for basement structures and infra-Cambrian salt distribution. GeoArabia. 2014; 19(1):85-112.
4. Al-Saadi HN, Baban EN. Introduction to the Gravity Exploration Method, Paiwand Press, Sulaimaniyah, Kurdistan Region, Iraq, 2014.
5. Alrefaee HA. Crustal modelling of the central part of the Northern Western Desert, Egypt using gravity data. Journal of African Earth Science. 2017; 129:72-81.
6. Chouhan AK. Structural fabric over the seismically active Kachchh rift basin, India: insight from world gravity model 2012. Environmental Earth Science. 2020; 79(13):1-14.
7. Chouhan AK, Singh D, Pal SK, Choudhury P. Delineation of subsurface geological fractures in the Cambay rift and surrounding regions of NW India: An integrated approach using satellite derived EIGEN-6C4 gravity data. Geocarto Int., 2020, 1-16.
8. Dim CIP, Onuoha KM, Okeugo CG, Ozumba BM. Petroleum system elements within the Late Cretaceous and Early Paleogene sediments of Nigeria's inland basins: An integrated sequence stratigraphic approach. Journal of African Earth Sciences. 2017; 130:76-86.
9. Dobrin MB. Introduction to geophysical prospecting. 4th edition, Mc-Graw Hill, UK, 2010.
10. Ekine AS, Onuoha MK. Burial History Analysis and Subsidence in the Anambra Basin, Nigeria. Department of Physics University of Port Harcourt, Nigeria; Department of Geology University of Nigeria, Nsukka, Nigeria, 2008. www.ajol.info.
11. Eke PO, Nelson SK. Subsurface Sedimentary Thickness and Structural types of Formations in Imo State, Nigeria, from Airborne Gravity Data. Asian Journal of Basic Science & Research. 2021; 3(4):1-8.
12. Igwe EA, Yakubu JA, Igboji IJ. Investigation of Nsukka Area, South-Eastern Nigeria for Mineral Exploration Using Gravity Method. Journal of Applied Physics (IOSR-JAP). 2018; 10(2):22-32.
13. International Gravimetric Bureau (Bureau Gravimétrique International, BGI) http://bgi.cnes.fr. Retrieved 12/2/2021.
14. Mariita NO. Application of Precision gravity

measurement to reservoir monitoring of Olkaria Geothermal Field. Proceedings world geothermal congress 2000, 2010, 2719-2724.
15. Njeudjang K, Essi JMA, Kana JD, Teikeu WA, Nouck PN, Djongyang N, Tchinda R. Gravity investigation of the Cameroon Volcanic Line in Adamawa region: geothermal features and structural control. Journal of African Earth Sciences 165, 2020:103809.
16. Obaje NG. Geology and Mineral Resources of Nigeria. Springer, 2009.
17. Obasi I, Selemo OAI, Nomeh JS. Gravity models as tool for basin boundary demarcation: A case study of Anambra Basin, Southeastern Nigeria. Journal of Applied Geophysics. 2017; 156:31-43.
18. Obi GC, Okagbue CO, Nwajide CS. Evolution of the Enugu Cuesta: A tectonically driven erosional process. Global Journal of Pure and Applied Science. 2001; 7:321-329.
19. Oboh-Ikuenobe FE, Obi CG, Jaramillo CA. Lithofacies, Palynofacies, and Sequence Stratigraphy of Palaeogene Strata in Southeastern Nigeria. J. Afr. Earth Sci. 2005; 41(1-2):79-101.
20. Odunze SO, Obi GC. Sedimentology and sequence stratigraphy of the Nkporo Group (Campanian-Maastrichtian), Anambra Basin, Nigeria. J Palaeogeogr. 2013; 2(2):192-208.
21. Oha AI, Onuoha, KM, Nwegbu, AN and Abba AU. Interpretation of high-resolution aeromagnetic data over southern Benue Trough, Southeastern Nigeria: Journal of Earth Systems Science. 2016; 125:369-385.
22. Okpoli CC. Delineation of high-resolution aeromagnetic survey of Lower Benue Trough for lineaments and mineralization: Case study of Abakaliki Sheet 303: Malaysian Journal of Geosciences. 2019; 3:51-60.
23. Olagundoye OO, Okereke CS, Edet AE, Obi D and Ukpong A. Depth to magnetic basement in the Anambra Basin, Benue Trough of Nigeria from aeromagnetic data: A prelude for hydrocarbon exploration, Interpretation. 2021; 9:SH11-SH26.
24. Olubayo LB. The main oil source formation of the Anambra Basin, south-eastern Nigeria, PhD thesis, geology department, university of Ibadan, Nigeria, 2016, 54-60.
25. Onuoha KM, Dim CIP. Prospects and Challenges of Developing Unconventional Petroleum Resources in The Anambra Inland Basin of Nigeria: Presented at the 2016 Africa Energy and Technology Conference, AAPG/SPE, 2016.
26. Onyekuru SO, Nwankwor GI, Akaolisa CZ. Chemical Characteristics of Groundwater Systems in the Southern Anambra Basin, Nigeria. Journal of Applied Sciences Research. 2010; 6(12):2164-2172.
27. Petit C, D´everch`ere J, Calais E, San'kov V, Fairhead D. Deep structure and mechanical behaviour of the lithosphere in the Hangai–H¨ovsg¨ol region, Mongolia: new constraints from gravity modelling. Earth Planet Sci. Lett. 2020; 197(3-4):133-149.
28. Prieto C. Gravity/magnetic signatures of various geologic models-an exercise in pattern recognition. IGC footnote series. 1996; 4(4):1-24.
29. Reid AB, Allsop JM, Thurston, JB. The structural index in gravity and magnetic Interpretation: Errors, uses and abuses. Geophysics. 2014; 79(4):61-66.
30. Selley RC, Sonnenberg SA. Elements of Petroleum Geology. 3rd Edition, Elsevier, Amsterdam. 2015; 507.
31. Tschirhart V, Jefferson CW, Morris WA. Basement geology beneath the northeast Thelon Basin, Nunavut: Insights from integrating new gravity, magnetic and geological data. Geophys. Prospect. 2017; 65(2):617-636.
32. Wang Y, Chen L, Yang G, Wu L, Xiao A, Zhou Y, *et al*. The late Paleoproterozoic to Mesoproterozoic rift system in the Ordos Basin and its tectonic implications: Insight from analyses of Bouguer gravity anomalies. Precambrian Res. 2021; 352:105964.
33. Zhang C, Chen J, Song M, Wang J, Yuan B. Structural interpretation of the Qingdongarea in Bohai Bay Basin from shipborne gravity data. Polish Maritime Research. 2015; 22:100-105.